

Direct Observation and Quantitative Analysis of Lithium Dendrite Growth by In Situ Transmission Electron Microscopy

To cite this article: Megan Diaz and Akihiro Kushima 2021 J. Electrochem. Soc. 168 020535

View the <u>article online</u> for updates and enhancements.

Discover the EL-CELL potentiostats

- Fully independent test channels with Pstat / GStat / EIS
- Optionally with integrated temperature controlled cell chamber
- Unique Connection Matrix: Switch between full-cell and half-cell control at runtime

www.el-cell.com +49 (0) 40 79012 734 sales@el-cell.com







Direct Observation and Quantitative Analysis of Lithium Dendrite Growth by In Situ Transmission Electron Microscopy

Megan Diaz¹ and Akihiro Kushima^{1,2,z}

In this work, a unique in situ transmission electron microscopy technique (TEM) was developed to evaluate the mechanical stress imposed at the lithium metal and the electrolyte interface during lithium dendrite growth. The method enables a direct observation of the lithium deposition process and the quantification of the mechanical stress associated with the dendritic growth of lithium metal. We successfully observed a nano-sized lithium dendrite nucleation/growth and quantified its pushing force during the process. The transition of the growth mode from a vertical direction to a parallel direction (relative to the solid electrolyte surface) after the compressive stress reached a threshold value was observed. The transition stress was much lower than the yield stress of nano-sized lithium and the stiffness of the solid electrolyte. The fundamental information obtained by this work gives useful insight towards designing a robust solid electrolyte necessary for all-solid-state lithium batteries.

© 2021 The Electrochemical Society ("ECS"). Published on behalf of ECS by IOP Publishing Limited. [DOI: 10.1149/1945-7111/abe5ec]

Manuscript submitted January 20, 2021; revised manuscript received February 9, 2021. Published February 23, 2021. This was paper 975 presented during PRiME 2020, October 4–9, 2020.

Supplementary material for this article is available online

Lithium ion batteries (LIBs) are the most widely-used energy storage devices in various applications including consumer electronics and electric vehicles (EVs). 1-3 However, with the current LIBs reaching their theoretical limits, the development of next generation energy storage technologies is crucial, particularly for highly demanding applications such as EVs. 4 Here, the lithium metal anode is attracting attention as an essential component in high energy density batteries. It has an extremely high theoretical capacity of 3800 mAh g^{-1} and a low electrochemical potential of -3.04 V with respect to the standard hydrogen potential. Despite significant efforts since the first invention of the lithium metal battery in 1970,⁵ practical applications of the lithium metal anode have yet to be successful. 1,2,6-The two major challenges are dendrites and electrolyte decomposition at the reactive lithium surface. Dendrite growth causes significant safety concerns when lithium metal anodes are combined with flammable liquid electrolytes used in LIBs. It becomes perilous when dendrites propagate through the electrolyte and contact the cathode leading to a short circuit of the cell and causing fire and even explosions. A significant number of works have been performed to mitigate the risks caused by dendrites. These approaches include; control of dendrites by forming a proper solid electrolyte interface (SEI) layer, ^{10,11} utilizing cations as a self-healing electrostatic shield mechanism, ¹² nanostructuring of the electrode¹³ and/or by the electrolyte, ¹⁴ and controlling the direction of growth for dendrites present in the electrolyte.¹

Another route is to introduce solid-state electrolytes (SSEs) with much higher modulus than lithium metal to effectively prevent the penetration of dendrites. 16,17 The use of SSEs (a combination of solid polymer and inorganic ceramic electrolytes) was reported to enable the use of a high capacity lithium metal anode without safety concerns. The benefits of using SSEs in the place of liquid electrolytes include increased theoretical cell energy/power density, a wide temperature range for operation, increased safety and a longer expected life cycle. It had been theorized that using a SSE with 2x the shear modulus of lithium can prevent the growth, or at least the propagation, of the dendrites. However, many studies involving SSEs with high shear moduli have revealed that the penetrations of dendrites still occur through SSEs. 22-26 The possible penetration routes may be along or through surface defects, 77 grain boundaries and interconnected open voids. 28,29 Different techniques have been

utilized to halt lithium dendrite growth such as grain boundary modification, eliminating surface defects or interconnected pores, and using SSEs with a large relative density. For example, $\text{Li}_{6.5}\text{La}_{32}\text{Zr}_{1.5}\text{Ta}_{0.5}\text{O}_{12}$ (LLZT) pellets modified with $\text{Li}_{2}\text{CO}_{3}$ and LiOH showed a high critical current density (CCD) before shorting at 0.6 mA cm⁻², while the unmodified pellets resulted in a short circuit at a lower CCD of 0.15 mA cm⁻². The modifications of the pellets acted as plugs in the SSE voids and caused sintering of LLZT, which prevented lithium dendrite growth through the SSE.

Despite the many techniques suggesting potential dendrite growth solutions through SSEs, there is very little understanding about the exact mechanism of dendrite penetration, especially at the initial stages of lithium dendrite growth. Knowing the stress conditions at the lithium/SSE interface during the electrochemical plating of lithium is crucial to discuss the mechanical stability of the SSEs and reveal how lithium penetrations occur. Interplays between mechanical and electrochemical interactions during the charge/ discharge process have been studied. 15-17 Sethuraman et al. found in their study of a graphite-based lithium-ion battery that the compressive stresses at the electrode of 1-2 MPa, which was attributed to binder swelling, culminated at a maximum of $10-12\,\mathrm{MPa}$ during intercalation. Which larger stress was observed for the Si electrode with large volume changes during charge/discharge processes. Chon et al. observed around 0.5 GPa of biaxial compressive stress during lithiation, and a tensile stress greater than 1.5 GPa was measured upon delithiation causing plastic deformation of the electrode. 31 On the other hand, lithium plating at the SSE/electrode interface involves complex electrochemical and mechanical processes. When dendrites are nucleated, they may impose stresses in nano- and atomic-scales at the interface. With a potentially high modulus and vield strength of lithium at nano-scales.³² the stress at the interface may well exceed the limit of the SSEs. In situ characterization techniques have been developed to quantify these electro-chemo-mechanics in battery electrodes and electrolytes.³² However, most of these techniques are measuring macroscopic ensembles and cannot extract information about the highly-localized events, which are important for understanding the failure of the SSEs and lithium penetrations.

In situ TEM is widely used to characterize electrochemical reactions^{36–39} and mechanical behaviors^{40–44} at nano-scales. However, the challenge still remains to characterize the electrochemo-mechanics at this resolution. In this work, we developed an in situ TEM technique that enables direct observation of dendrite

¹Department of Materials Science and Engineering, University of Central Florida, Orlando, Florida 32816, United States of America

²Advanced Materials Processing and Analysis Center, and NanoScience Technology Center, University of Central Florida, Orlando, Florida 32816, United States of America

nucleation and growth on the nano-scale and quantitative analysis of the stress evolution during the growth process.

Experimental and Modeling

In situ transmission electron microcsopy.—The in situ experiment was conducted in an FEI TALOS F200X Operando S/TEM equipped with an X-FEG electron source at an operating voltage of 200 kV. The experimental setup is shown schematically in Fig. 1. Inside a glovebox, solid Li metal was prepared by scraping the surface with a blade to remove any possible oxidation from its surface. A conductive atomic force microscopy (AFM) cantilever (Bruker SCM-PIC) was attached to a gold rod using conductive epoxy, and lithium metal was deposited onto the tip of a W rod by directly scratching it against the prepared Li metal. The two rods were mounted on a Nanofactory scanning tunneling microscopy (STM)-TEM holder inside the glovebox. The holder is equipped with a piezo manipulator and has a biasing capability, which allows for a controlled approach of the cantilever tip to contact the lithium metal surface for lithium deposition. The TEM holder was sealed when transferred to the TEM to minimize the atmompheric exposure of the Li metal (<2 s during the insertion of the holder). The surface of the Li metal was instantaneously oxidized to form a thin layer of Li₂O, which was used as a solid electrolyte. 45-47 This solid electrolyte surface was located and contacted by the cantilever inside the TEM. Finally, a potential was applied to initiate the growth of lithium causing displacement of the AFM cantilever. Image analysis was performed to obtain the relationship between the change in the dendrite geometry and the displacement of the cantilever tip. During the experiment, the electron beam dosage was carefully controlled to minimize the beam effect on the observed dendrite growth, and no dendrite nucleation occurred without biasing.

Ab initio simulation.—The calculation of the ad-atom and the vacancy formation energies on the lithium surface was conducted using Vienna Ab-initio Simulation Package (VASP). The simulation slab model consisted of 48 li atoms with x, y, and z axis corresponding to [110], $[\bar{1}10]$, and [001] direction, respectively. The model contained six (001) layers and 10 Å of the vacuum layer to calculate the surface state. First, bulk simulation model was created, applied different compressive strains along [110] direction, and the structural optimization was performed by relaxing the atom positions and the cell parameter except for the compressed axis for each strain. Using the obtained cell parameter, the surface model was created for zero-strain and compressed surface models. The surface atomic structures were relaxed with the bottom two atom layers fixed. The ad-atom and the vacancy were created by placing an Li atom on a surface lattice point and removing it from the top layer, followed by the structural relaxation. Finally, the ad-atom/vacancy formation energies at different compression strains were calculated by $E_{\rm ad}-E_{\rm B}-E_{\rm 0}$ for ad-atom and $E_{\rm vac}$ + $E_{\rm B}-E_{\rm 0}$ for vacancy. Here, $E_{\rm ad}$ is the energy of the surface model with an ad-atom, $E_{\rm vac}$ is the one with a vacancy, $E_{\rm B}$ is the energy/atom in bulk, and E_0 is the energy of the surface model without ad-atom/ vacancy. In the calculation, plane-wave energy cut-off of 600 eV and the generalized gradient approximation (GGA) parameterized by Perdew, Burke and Ernzerhof⁵⁰ were used for the exchange-correlation functional, and the ionic core was represented with projected-augumented wave (PAW) potential. ^{51,52} A $7\times7\times9$ and $3\times3\times1$ Monkhorst-Pack⁵³ k-point mesh were selected for the bulk and the surface model, respectively.

Results and Discussion

The process of lithium growth observed by the in situ TEM is depicted in Fig. 2 (see Supplementary Information Movie S1 available online at stacks.iop.org/JES/168/020535/mmedia). After the potential of -2.0 V was applied to the cantilever with respect to the counter electrode, the lithium dendrite started to grow vertically,

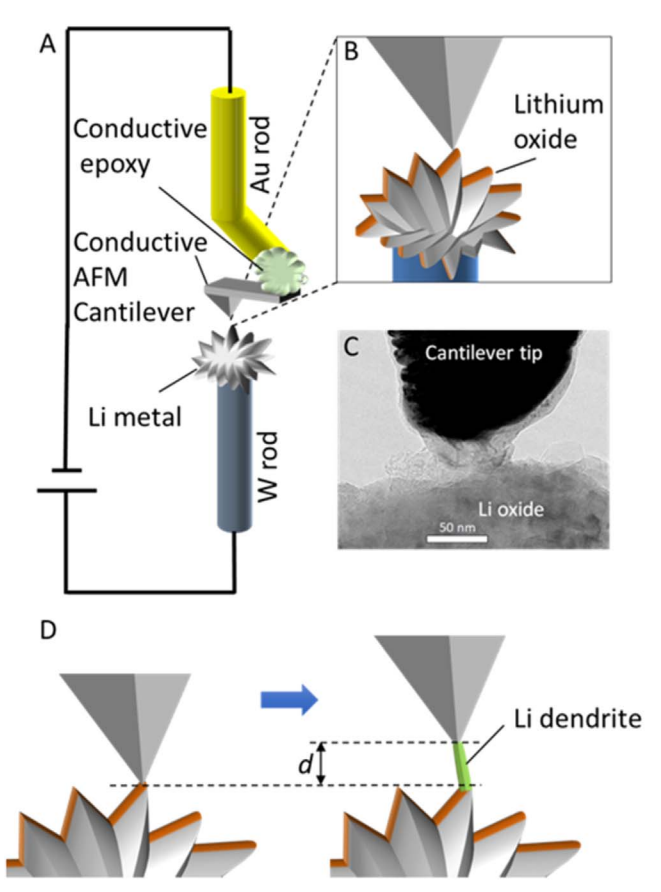


Figure 1. (A) Schematic illustration of the in situ TEM set up showing the AFM cantilever attached to a gold rod via a conductive epoxy approaching lithium metal on a tungsten rod. (B) Magnified view of the cantilever approaching the lithium metal/lithium oxide surface. (C) TEM image of cantilever tip contacting lithium oxide. (D) Schematic of cantilever displacement due to lithium dendrite growth upon application of a potential.

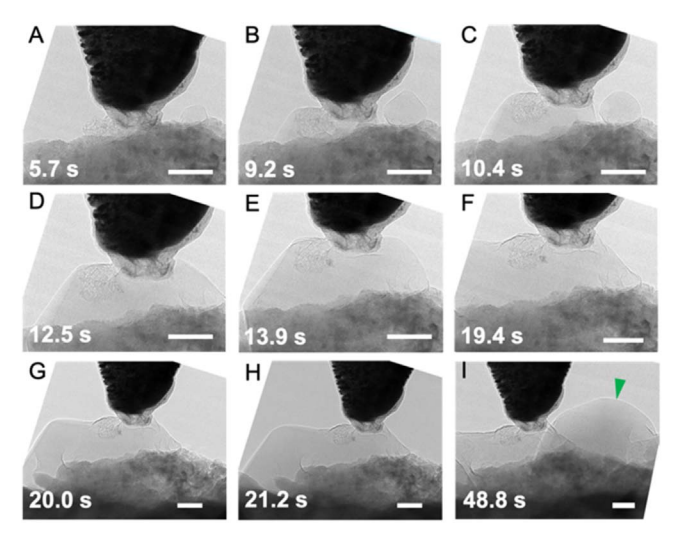


Figure 2. TEM micrographs depicting lithium dendrite growth displacing cantilever. Time stamps, in seconds, denote the amount of time passed since initial displacement of cantilever. Image I reveals uninhibited lithium growth (denoted by a green triangle) surpassing the height of the lithium under the cantilever. Scale bar is 50 nm.

pushing the cantilever away from the surface. After 13.9 s of vertical cantilever deflection, the vertical growth ceased and horizontal growth became the primary direction of lithium dendrite propagation.

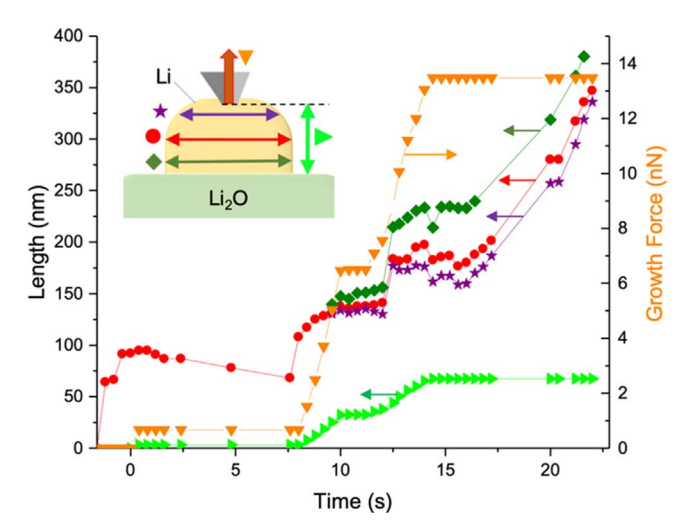


Figure 3. Temporal evolution of the dendrite geometry and the growth force. The widths and height are defined in the inset. Widths are measured at three different locations, top (purple star), center (red circle) and bottom (dark green diamond). The top and the bottom were measured 10 nm from the cantilever tip and the dendrite base, respectively. The height (lime green arrow) was measured from the base of the dendrite to the cantilever tip. The orange upside-down triangle line represents growth force calculated from the deflection of the cantilever. Time zero indicates initiation of cantilever tip deflection by the dendrite.

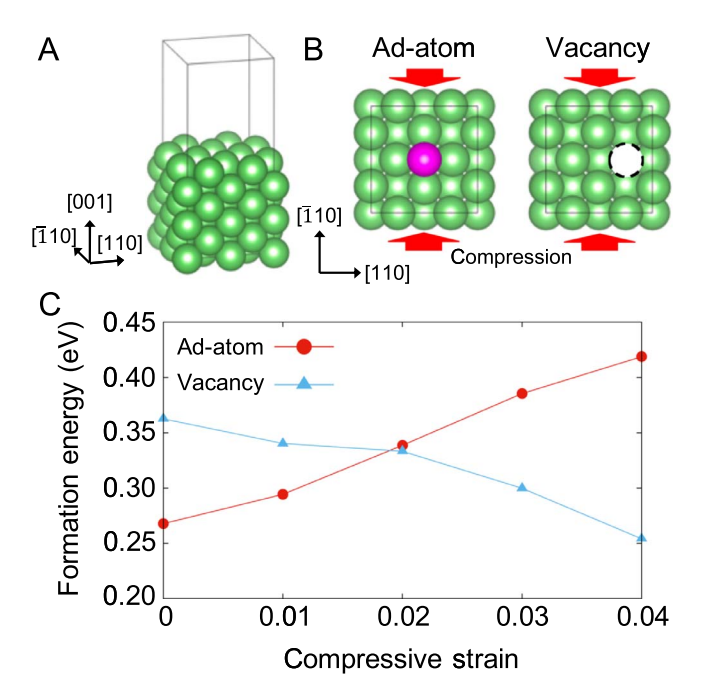


Figure 4. (A) Simulation model of Li (001) surface. (B) Ad-atom/vacancy created on the surface to calculate the change in the formation energy under compressive stress along [110] direction. (C) Relationships between the adatom/vacancy formation energies and the compressive strain.

Figure 3 shows the change in lithium dendrite geometry during the growth and resulting force, $F_{\rm Li}$, on the dendrite pushing against the cantilever. The force was calculated by Hook's law $F_{\rm Li}=kx$, where k is the spring constant of the cantilever and x is the displacement. A small force is observed at the beginning corresponding to the nucleation of the dendrite. The force increased as it grew, pushing the cantilever away from the surface, and reached its maximum value of 13.5 nN. Assuming a circular contact between the cantilever tip and the dendrite surface, the maximum stress

imposed at the top of the dendrite is calculated to be 15.8 MPa. After this critical stress, the lithium pillar stopped growing in the height direction and started to grow in the width direction. The maximum stress observed, 15.8 MPa, is much larger than the reported bulk polycrystalline lithium elastic yield stress value range (0.41 to 0.89 MPa). $^{32.54}$ However, this value is still lower than the yield stress of a 1 μ m sized lithium pillar of $\sim\!100$ MPa. 32 Therefore, under different growth conditions, the lithium pillar has the potential to grow higher without yielding. The lithium growth direction then changed as the dendrite stopped displacing the cantilever and instead expanded horizontally. A stresss-reducing driving force may have caused this preferential horizontal growth before the ultimate yield stress of the dendrite was reached. Unobstructed lithium, indicated by the arrowhead in Fig. 2I, freely grew in both the horizontal and vertical directions past the maximum height of the dendrite that was restricted by the cantilever.

Change in the growth direction of the dendrite can be affected by the thermodynamics at the surface. To clarify the effect of the compressive stress, the ad-atom and vacancy formation energies were studied by first principles calculations. A compressive stress was applied along the [110] direction and the ad-atom and vacancy formation energies on the [001] surface were calculated. The results are shown in Fig. 4. With the increasing compressive stress, the adatom formation energy was increased from 0.27 to 0.42 eV atom⁻¹ and the vacancy formation energy was decreased from 0.36 to 0.23 eV atom⁻¹. This indicates the surface lithium atoms have a tendency to flow away from highly compressed areas and relax the stress, which agrees with the experimental observation.

Figure 5 shows a schematic of the three different stages of lithium dendrite growth. The first stage is the nucleation where the seed of dendrite emerges at the contact between the electrolyte and the electrode. The second stage is vertical dendrite growth in which the cantilever was displaced as the growth force increased. The third stage is the horizontal dendrite growth after reaching the vertical growth limit, where the dendrite increased its growth rate in the horizontal direction due to its inability to vertically displace the cantilever. When considering how the dendrite grew, two mechanisms are presented. One is the diffusion of Li⁺ ions from the electrolyte towards the root of the dendrite where it recombines with an electron to form metallic lithium. Another process that may be taking place simultaneously is the diffusion of lithium atoms from the side of the dendrite to the tip. Our observation depicted the former as the primary growth mode as there were no changes in the morphology at the contact between the cantilver tip and the dendrite. The occasional decrease of the dendrite width seen in Fig. 3, particularly at the top part, can be explained by the stress-driven surface atom diffusion predicted by the simulation as shown in Fig. 4.

A similar in situ TEM study of the lithium dendrite growth force was reported by He, et al., where the sharp lithium whisker (dendrite) grew until buckling occurred when the stress reached \sim 100 MPa. The difference from the observation in this work may be attributed to the difference in the geometry of the electrodeelectrolyte contact. The reported work by He et al. has a flat cantilever tip (current collector) contacting a sharp solid electrolyte at the lithium surface, as opposed to our setup, where a sharp cantilever tip contacted a relatively flat region of the solid electrolyte. The sharp cantilever contact restricted the electrical current flow but enhanced the lithium ion supply through a large solid electrolyte surface. This allowed ample supply of lithium ions to promote side-ways growth of the dendrite at a much lower stress than the yield or buckling stress. It is clear that decreasing roughness at the electrode-electrolyte interface is desired for stable lithium deposition/stripping cycles.⁵⁶ Our direct measurement of the stress that causes the transition in the dendrite growth direction indicates the stress above 16 MPa is required to guide the lithium dendrite growth in the horizontal direction to promote conformal contact between lithium and solid electrolyte, which agrees with a model prediction.⁵⁷ Although a sharp electrode contact may cause a high

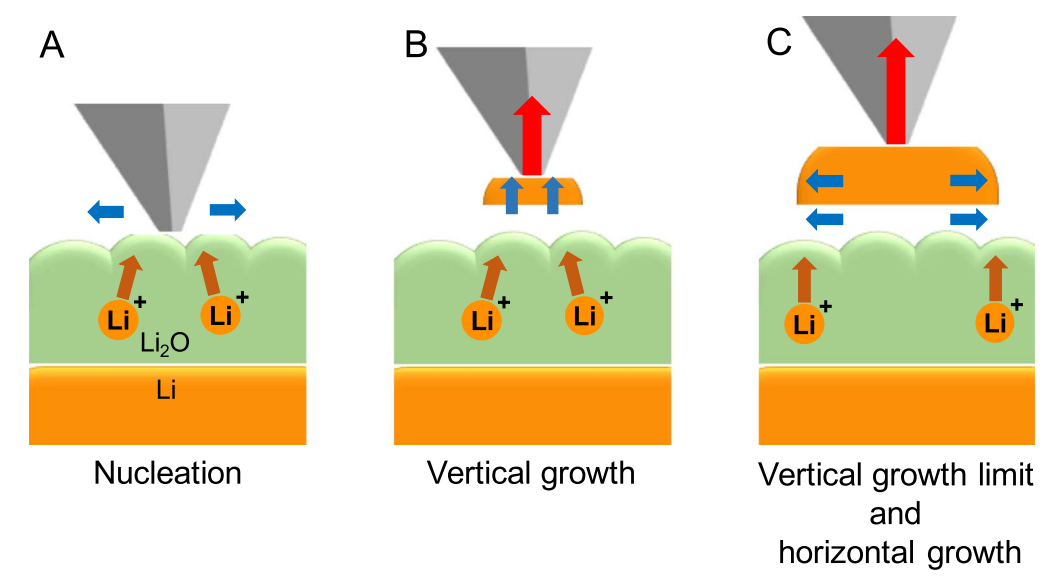


Figure 5. Schematic illustration of the Li dendrite nucleation and growth process observed in this work. (A) Nucleation of the dendrite. (B) Vertical dendrite growth, deflecting the cantilever. (C) The dendrite's horizontal growth increases rapidly after reaching the maximum vertical growth force.

electric field concentration promoting dendrite growth on the spot, the growth direction may be guided towards the side-ways growth instead of the detrimental vertical growth that increases stress concentration leading to the buckling of dendrites or even electrolyte fracture.

The maximum possible pressure measured in this study of the lithium dendrite growth was 15.8 MPa, which can be accommodated by only $\sim 0.01\%$ strain using typical solid electrolyte materials with high Young's modulus as follows: 58 Li_{0.33}La_{0.57}TiO₃, 186 to 200 GPa; Li₇La₃Zr₂O₁₂, 150 GPa; and Li_{1+x+y}Al_xTi_{2-x}Si_yP_{3-y}O₁₂, 119 GPa, which should have enough tolerance against Li penetrations provided they do not have critical defects or grain boundaries. However, in many cases Li dendrite penetrations can still take place in SSEs, $^{22-26}$ and Li₇La₃Zr₂O₁₂ is specifically reported to suffer from dendrite penetration. ⁵⁹ The result of our experiment supports theories suggesting dendrite growth through defects and grain boundaries, or Han et al.'s process describing dendrite formation that occurred via recombination of electrons and lithium ions due to electron migration through the SSE.⁶⁰ It implies that a key for developing practical all-solid-state lithium batteries is to control the defects and grain boundaries in order to eliminate any weak spots in the SSEs that lead to the catastrophic failure of the device.

The in situ TEM dendrite growth force measurement provided crucial information for understanding the fundamental mechanisms behind the lithium dendrite growth. The quantitative stress values associated with the dendrite growth behavior obtained in this work can be useful in the selection of solid-state electrolytes with properties that inhibit dendrite propagations. The observation also suggests contact geometries can be a key for controlling the growth direction.

Acknowledgments

The authors thank Dong Su, Sooyeon Hwang, and Kim Kisslinger from Brookhaven National Laboratory. This research used resources of the Center for Functional Nanomaterials, which is a U.S.DOE Office of Science Facility, at Brookhaven National Laboratory under Contract DE-SC0012704. This work was supported by the National Science Foundation under Grant No. CMMI-1942554.

ORCID

References

- 1. D. Aurbach, E. Zinigrad, Y. Cohen, and H. Teller, "A short review of failure mechanisms of lithium metal and lithiated graphite anodes in liquid electrolyte solutions." Solid State Ionics, 148, 405 (2002).
- M. S. Whittingham, "History, evolution, and future status of energy storage." Proc. IEEE, 100, 1518 (2012).
- 3. M. Armand and J.-M. Tarascon, "Building better batteries." Nature, 451, 652 (2008).
- 4. R. V. Noorden, "The rechargeable revolution: A better battery chemists are reinventing rechargeable cells to drive down costs and boost capacity." Nature, 507, 26 (2014).
- M. S. Whittingham, "Electrical energy storage and intercalation chemistry." Science, **192**, 1126 (1976).
- 6. D. Aurbach and Y. Cohen, "The application of atomic force microscopy for the study of li deposition processes." *J. Electrochem. Soc.*, **143**, 3525 (1996). W. Xu, J. Wang, F. Ding, X. Chen, E. Nasybulin, Y. Zhang, and J.-G. Zhang,
- "Lithium metal anodes for rechargeable batteries." Energy Environ. Sci., 7, 513
- 8. Z. Li, J. Huang, B. Yann Liaw, V. Metzler, and J. Zhang, "A review of lithium deposition in lithium-ion and lithium metal secondary batteries." J. Power Sources, **254**. 168 (2014)
- 9. C. Hendricks, N. Williard, M. Sony, and M. Pecht, "A failure modes, mechanisms, and effects analysis (FMMEA) of lithium-ion batteries elsevier enhanced reader." I. Power Sources, 297, 113 (2015).
- 10. G. Wan, F. Guo, H. Li, Y. Cao, X. Ai, J. Qian, Y. Li, and H. Yang, "Suppression of dendritic lithium growth by in Situ formation of a chemically stable and mechanically strong solid electrolyte interphase." ACS Appl. Mater. Interfaces, 10, 593 (2018).
- 11. X.-B. Cheng, R. Zhang, C.-Z. Zhao, F. Wei, J.-G. Zhang, and Q. Zhang, "A review of solid electrolyte interphases on lithium metal anode." Adv. Sci., 3, 1500213
- 12. F. Ding et al., "Effects of cesium cations in lithium deposition via self-healing electrostatic shield mechanism." The Journal of Physical Chemistry C., 118, 4043
- 13. X.-B. Cheng, H.-J. Peng, J.-Q. Huang, R. Zhang, C.-Z. Zhao, and Q. Zhang, "Dualphase lithium metal anode containing a polysulfide-induced solid electrolyte interphase and nanostructured graphene framework for lithium-sulfur batteries. ACS Nano., 9, 6373 (2015).
- 14. L. Li, S. Li, and Y. Lu, "Suppression of dendritic lithium growth in lithium metalbased batteries." Chem. Commun., 54, 6648 (2018).
- 15. P. Zou, Y. Wang, S.-W. Chiang, X. Wang, F. Kang, and C. Yang, "Directing lateral growth of lithium dendrites in micro-compartmented anode arrays for safe lithium metal batteries." Nat. Commun., 9, 464 (2018).
- 16. J. Janek and W. G. Zeier, "A solid future for battery development." Nat. Energy, 1, 16141 (2016).
- 17. K. Kerman, A. Luntz, V. Viswanathan, Y.-M. Chiang, and Z. Chen, "Reviewpractical challenges hindering the development of solid state li ion batteries." J. Electrochem. Soc., 164, A1731 (2017).
- 18. H. Duan, Y.-X. Yin, Y. Shi, P.-F. Wang, X.-D. Zhang, C.-P. Yang, J.-L. Shi, R. Wen, Y.-G. Guo, and L.-J. Wan, "Dendrite-free li-metal battery enabled by a thin asymmetric solid electrolyte with engineered layers." JACS, 140, 82 (2018).
- 19. A. Manthiram, X. Yu, and S. Wang, "Lithium battery chemistries enabled by solidstate electrolytes." *Nature Reviews Materials.*, **2**, 16103 (2017).

 20. C. Monroe and J. Newman, "The effect of interfacial deformation on electro-
- deposition kinetics." J. Electrochem. Soc., 151, A880 (2004).

- C. Monroe and J. Newman, "The impact of elastic deformation on deposition kinetics at lithium/polymer interfaces." J. Electrochem. Soc., 152, A396 (2005).
- R. Sudo, Y. Nakata, K. Ishiguro, M. Matsui, A. Hirano, Y. Takeda, O. Yamamoto, and N. Imanishi, "Interface behavior between garnet-type lithium-conducting solid electrolyte and lithium metal." *Solid State Ionics*, 262, 151 (2014).
- Y. Suzuki, K. Kami, K. Watanabe, A. Watanabe, N. Saito, T. Ohnishi, K. Takada, R. Sudo, and N. Imanishi, "Transparent cubic garnet-type solid electrolyte of Al2O3-doped Li7La3Zr2O12." Solid State Ionics, 278, 172 (2015).
- A. Sharafi, H. M. Meyer, J. Nanda, J. Wolfenstine, and J. Sakamoto, "Characterizing the Li-Li₇La₃Zr₂O₁₂ interface stability and kinetics as a function of temperature and current density." *J. Power Sources*, 302, 135 (2016).
- F. Aguesse, W. Manalastas, L. Buannic, J. M. Lopez del Amo, G. Singh, A. Llordés, and J. Kilner, "Investigating the dendritic growth during full cell cycling of garnet electrolyte in direct contact with li metal." ACS Appl. Mater. Interfaces, 9, 3808 (2017).
- R. H. Basappa, T. Ito, and H. Yamada, "Contact between garnet-type solid electrolyte and lithium metal anode: influence on charge transfer resistance and short circuit prevention." J. Electrochem. Soc., 164, A666 (2017).
- L. Porz, T. Swamy, B. W. Sheldon, D. Rettenwander, T. Frömling, H. L. Thaman, S. Berendts, R. Uecker, W. C. Carter, and Y.-M. Chiang, "Mechanism of lithium metal penetration through inorganic solid electrolytes." *Adv. Energy Mater.*, 7, 1701003 (2017).
- Y. Ren, Y. Shen, Y. Lin, and C.-W. Nan, "Direct observation of lithium dendrites inside garnet-type lithium-ion solid electrolyte." *Electrochem. Commun.*, 57, 27 (2015).
- R. Hongahally Basappa, T. Ito, T. Morimura, R. Bekarevich, K. Mitsuishi, and H. Yamada, "Grain boundary modification to suppress lithium penetration through garnet-type solid electrolyte." *J. Power Sources*, 363, 145 (2017).
- V. A. Sethuraman, N. V. Winkle, D. P. Abraham, A. F. Bower, and P. R. Guduru, "Real-time stress measurements in lithium-ion battery negative-electrodes." *J. Power Sources*, 206, 334 (2012).
- M. J. Chon, V. A. Sethuraman, A. McCormick, V. Srinivasan, and P. R. Guduru, "Real-time measurement of stress and damage evolution during initial lithiation of crystalline silicon." *Phys. Rev. Lett.*, 107, 045503 (2011).
- C. Xu, Z. Ahmad, A. Aryanfar, V. Viswanathan, and J. R. Greer, "Enhanced strength and temperature dependence of mechanical properties of Li at small scales and its implications for Li metal anodes." *PNAS*, 114, 57 (2017).
- V. A. Sethuraman, V. Srinivasan, A. F. Bower, and P. R. Guduru, "In Situ measurements of stress-potential coupling in lithiated silicon." J. Electrochem. Soc., 157, A1253 (2010).
- V. A. Sethuraman, M. J. Chon, M. Shimshak, V. Srinivasan, and P. R. Guduru, "In situ measurements of stress evolution in silicon thin films during electrochemical lithiation and delithiation." *J. Power Sources*, 195, 5062 (2010).
- X. Cheng and M. Pecht, "In situ stress measurement techniques on li-ion battery electrodes: a review." *Energies.*, 10, 591 (2017).
- J. Y. Huang et al., "In situ observation of the electrochemical lithiation of a single SnO₂ nanowire electrode." *Science*, 330, 1515 (2010).
- A. Kushima, X. H. Liu, G. Zhu, Z. L. Wang, J. Y. Huang, and J. Li, "Leapfrog cracking and nanoamorphization of ZnO nanowires during In situ electrochemical lithiation." *Nano Lett.*, 11, 4535 (2011).
- Z.-H. Xie, Z. Jiang, and X. Zhang, "Review—promises and challenges of In situ transmission electron microscopy electrochemical techniques in the studies of lithium ion batteries." J. Electrochem. Soc., 164, A2110 (2017).
- N. Hodnik, G. Dehm, and K. J. J. Mayrhofer, "Importance and challenges of electrochemical in situ liquid cell electron microscopy for energy conversion research." ACS., 49, 2015 (2019).

- G. Richter, K. Hillerich, D. S. Gianola, R. Mönig, O. Kraft, and C. A. Volkert, "Ultrahigh strength single crystalline nanowhiskers grown by physical vapor deposition." *Nano Lett.*, 9, 3048 (2009).
- D. Zhang, J. Breguet, R. Clavel, V. Sivakov, S. Christiansen, and J. Michler, "In situ electron microscopy mechanical testing of silicon nanowires using electrostatically actuated tensile stages." *J. Microelectromech. Syst.*, 19, 663 (2010).
- A. M. Beese, D. Papkov, S. Li, Y. Dzenis, and H. D. Espinosa, "In situ transmission electron microscope tensile testing reveals structure-property relationships in carbon nanofibers." *Carbon*, 60, 246 (2013).
- J. Wang, Z. Zeng, C. R. Weinberger, Z. Zhang, T. Zhu, and S. X. Mao, "In situ atomic-scale observation of twinning-dominated deformation in nanoscale bodycentred cubic tungsten." *Nature Mater.*, 14, 594 (2015).
- A. Pandey, "In situ mechanical testing in electron microscopes: current progress and future opportunities in small-scale experimentation." JOM, 67, 1682 (2015).
- C.-M. Wang, "In situ transmission electron microscopy and spectroscopy studies of rechargeable batteries under dynamic operating conditions: a retrospective and perspective view." J. Mater. Res., 30, 326 (2015).
- M. M. Islam and T. Bredow, "Density functional theory study for the stability and ionic conductivity of Li₂O surfaces." J. Phys. Chem. C, 113, 672 (2009).
- F. Wang, H.-C. Yu, M.-H. Chen, L. Wu, N. Pereira, K. Thornton, A. Van der Ven, Y. Zhu, G. G. Amatucci, and J. Graetz, "Tracking lithium transport and electrochemical reactions in nanoparticles." *Nat. Commun.*, 3, 1201 (2012).
- G. Kresse and J. Hafner, "Ab initio molecular dynamics for liquid metals." Phys. Rev. B. 47, 558 (1993).
- G. Kresse and J. Furthmüller, "Efficient iterative schemes for ab initio total-energy calculations using a plane-wave basis set." Phys. Rev. B, 54, 11169 (1996).
- J. P. Perdew, K. Burke, and M. Ernzerhof, "Generalized gradient approximation made simple." *Phys. Rev. Lett.*, 77, 3865 (1996).
- G. Kresse and D. Joubert, "From ultrasoft pseudopotentials to the projector augmented-wave method." *Phys. Rev. B*, 59, 1758 (1999).
- 52. P. E. Blöchl, "Projector augmented-wave method." *Phys. Rev. B*, **50**, 17953 (1994).
- H. J. Monkhorst and J. D. Pack, "Special points for Brillouin-zone integrations." *Phys. Rev. B*, 13, 5188 (1976).
- S. Tariq, K. Ammigan, P. Hurh, R. Schultz, P. Liu, and J. Shang, "Li material testing- fermilab antiproton source lithium collection lens," 2003 Particle Accelerator Conference, Portland, OR, USA, May 2003 (2003).
- Y. He, X. Ren, Y. Xu, M. H. Engelhard, X. Li, J. Xiao, J. Liu, J.-G. Zhang, W. Xu, and C. Wang, "Origin of lithium whisker formation and growth under stress." *Nat. Nanotechnol.*, 14, 1042 (2019).
- S. Wang, J. Wang, J. Liu, H. Song, Y. Liu, P. Wang, P. He, J. Xu, and H. Zhou, "Ultra-fine surface solid-state electrolytes for long cycle life all-solid-state lithium-air batteries." *J. Mater. Chem. A*, 6, 21248 (2018).
- X. Zhang, Q. J. Wang, K. L. Harrison, S. A. Roberts, and S. J. Harris, "Pressuredriven interface evolution in solid-state lithium metal batteries." *Cell Reports Physical Science.*, 1, 100012 (2020).
- Y. H. Cho, J. Wolfenstine, E. Rangasamy, H. Kim, H. Choe, and J. Sakamoto, "Mechanical properties of the solid Li-ion conducting electrolyte: Li0.33La0.57TiO3." *J. Mater. Sci.*, 47, 5970 (2012).
- H.-K. Tian, B. Xu, and Y. Qi, "Computational study of lithium nucleation tendency in Li₇La₃Zr₂O₁₂ (LLZO) and rational design of interlayer materials to prevent lithium dendrites |Elsevier enhanced reader." J. Power Sources, 392, 79 (2018).
- F. Han, A. S. Westover, J. Yue, X. Fan, F. Wang, M. Chi, D. N. Leonard, N. J. Dudney, H. Wang, and C. Wang, "High electronic conductivity as the origin of lithium dendrite formation within solid electrolytes." *Nat. Energy*, 4, 187 (2019).